Title

Analysis of PV Module Power Loss and Cell Crack Effects Due to Accelerated Aging Tests and Field Exposure

Journal

IEEE Journal of Photovoltaics, 13(1)

ISSN

2156-3381

Authors

Libby, Cara

Paudyal, Bijaya

Chen, Xin

et al.

Publication Date

2023

DOI

10.1109/jphotov.2022.3228104

Analysis of PV Module Power Loss and Cell Crack Effects Due to Accelerated Aging Tests and Field Exposure

Cara Libby, *Member, IEEE*, Bijaya Paudyal, *Member, IEEE*, Xin Chen, William B. Hobbs, *Member, IEEE*, Daniel Fregosi, and Anubhav Jain

***Abstract*—This study compared module power loss for 36 modules that endured various accelerated aging test sequences before installation outdoors on a 10-kWp array in Birmingham, AL, USA for 1.72 to 2.72 years. Twelve modules endured standard IEC 61215 aging tests and 24 endured Qualification Plus (Qual Plus). Modules in each group were further split into two test sequences with different exposures. Electrical parameter variations were analyzed as a function of aging test and field exposure history. Fill factor loss was determined to be the cause of observed decreases in power output during accelerated aging tests, while decreases in both open circuit voltage and fill factor dominated the power loss during subsequent on-sun testing. Quantified cell crack features were extracted via computer vision tools from electroluminescence images and correlated with power loss. Results illustrate that standard aging tests led to negligible cracks, while Qual Plus test sequences yielded more severe cracks. While correlating results from qualification tests with in-field performance degradation parameters remains a challenge, this study provides new insights on specific environmental stressors and crack features that may play a role in power loss. Insights on accelerated aging protocols are discussed.**

***Index Terms*—Accelerated testing, cell cracks, degradation, performance, photovoltaic (PV).**

Manuscript received 6 October 2022; accepted 1 December 2022. Date of publication 21 December 2022; date of current version 12 January 2023. This work was supported in part by the U.S. Department of Energy's Office of Energy Efficiency and Renewable Energy under Solar Energy Technologies Office Agreement DE-EE0007137, in part by the National Renewable Energy Laboratory, operated by Alliance for Sustainable Energy, LLC, for the U.S. Department of Energy under Contract DE-AC36-08GO28308, and in part by the Durable Module Materials Consortium (DuraMAT)x an Energy Materials Network Consortium funded by the U.S. Department of Energy, Office of Energy Efficiency and Renewable Energy, Solar Energy Technologies Office. *(Cara Libby, Bijaya Paudyal, and Xin Chen are co-first authors.) (Corresponding author: Cara Libby.)*

Cara Libby is with the Electric Power Research Institute, Palo Alto, CA 94304 USA (e-mail: clibby@epri.com).

Bijaya Paudyal was with the Electric Power Research Institute, Charlotte, NC 28262 USA. He is now with the Enel Green Power, Charlotte, NC 28262 USA (e-mail: bijaya.paudyal@gmail.com).

Xin Chen is with the Lawrence Berkeley National Laboratory, Berkeley, CA 94720 USA (e-mail: chenxin0210@lbl.gov).

William B. Hobbs is with the Southern Company, Birmingham, AL 35203 USA (e-mail: whobbs@southernco.com).

Daniel Fregosi is with the Electric Power Research Institute, Charlotte, NC 28262 USA (e-mail: dfregosi@epri.com).

Anubhav Jain is with the Lawrence Berkeley National Laboratory, Berkeley, CA 94720 USA (e-mail: ajain@lbl.gov).

Color versions of one or more figures in this article are available at https://doi.org/10.1109/JPHOTOV.2022.3228104.

Digital Object Identifier 10.1109/JPHOTOV.2022.3228104

I. Introduction

THE solar photovoltaic (PV) testbed at the Southeastern Solar Research Center (SSRC) in Birmingham, AL, USA hosted a nominal 10-kWp array as part of a 2015–2018 U.S. Department of Energy (DOE)-funded study called Physics of Reliability: Evaluating Design Insights for Component Technologies in Solar 2 (PREDICTS2) [1]. A large, commercial PV power plant in the U.S. Southwest provided 36 pristine-condition spare modules for accelerated testing. The 72-cell multicrystalline silicon (c-Si) Al-BSF PREDICTS2 modules were sourced from the same manufacturer in 2012. Upon arrival at the SSRC, the modules were split into four groups that endured different laboratory-controlled accelerated aging test sequences: IEC 61215 and Qualification Plus (Qual Plus). Environmental stressors included thermal cycling (TC), humidity freeze (HF), and dynamic mechanical loading (DML). As batches of modules completed the aging tests, they were installed on a fixed, south-facing, 30°-tilt array, as shown in Fig. 1. When the system was decommissioned in mid-2020, module "on-sun" exposure durations ranged from 1.72 to 2.72 years. Each accelerated-aged module was connected to the grid via microinverter.

Capabilities developed in a separate Durable Module Materials Consortium (DuraMAT) study funded by DOE in 2019–2022 enabled quantification of crack features and correlation with changes in module electrical parameters and isolated cell areas. Electroluminescence (EL) images were used to assess cell crack features and isolated cell areas. Module power loss and electrical parameter variations were determined based on current–voltage (I–V) measurement data. The analysis considered differences in accelerated aging test history and length of outdoor field exposure in a humid subtropical climate.

II. Background

Qualification standards tests for PV modules are intended to certify the module design and bill of materials to avoid design flaws and early failures in the field. The consensus-based standards from the International Electrotechnical Commission (IEC), IEC 61215 series [2], are widely adopted for qualifying PV modules. The qualification tests are based on accelerated aging with different sequences designed specifically to clarify one or more degradation causes in a PV module. The accelerated aging test protocols reveal deficiencies in PV module design and

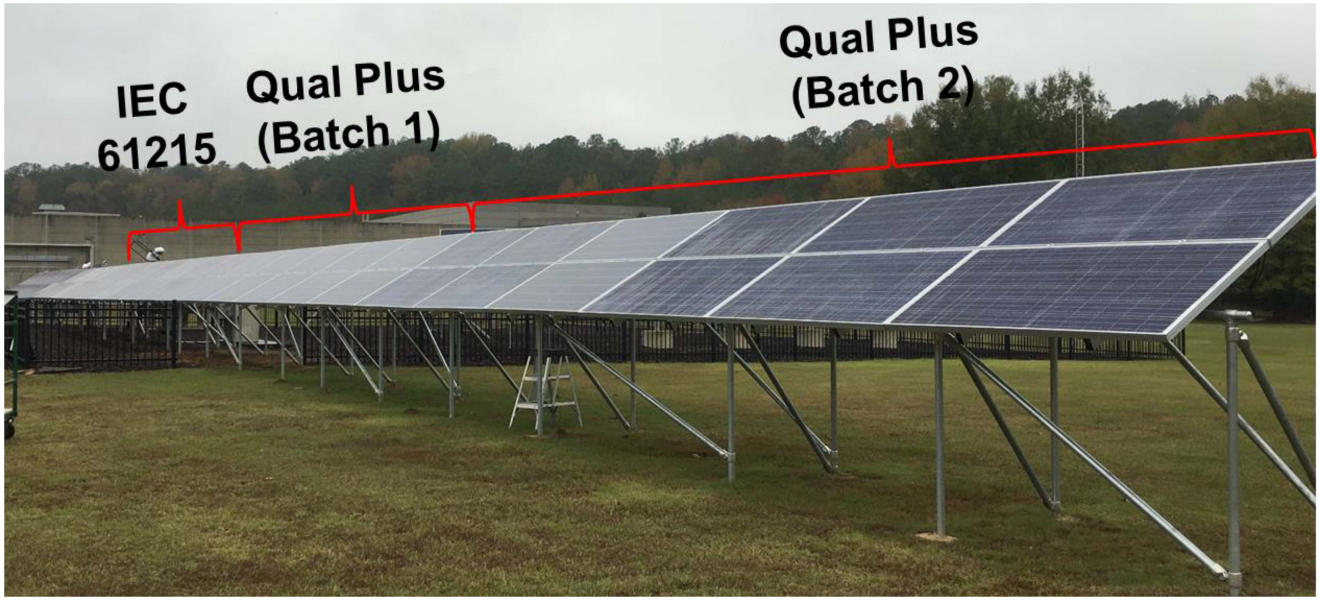

Fig. 1. PREDICTS2 modules installed outdoors in Birmingham, AL, USA.

material quality [3]; however, they are not intended to identify possible failure modes during field operation.

PV modules typically undergo the combined effect of multiple environmental stressors in the field – such as ultraviolet (UV) light exposure, thermal cycling, humidity, and wind loading – and exhibit a gradual drop in performance known as degradation. The degradation rate is a key parameter for estimating lifetime energy output and a PV system's payback period. Accelerated lifetime test results are insufficient to determine the gradual performance loss of PV modules in an outdoor environment. Previous studies have revealed that failure modes such as corrosion of cells and busbars, discoloration, and delamination of the encapsulant materials contributing to the degradation of PV modules in the field are rather different from the degradation and failure modes observed in accelerated tests [4]. Several recommendations have been made to extend accelerated test protocols from the baseline IEC 61215 (design qualification and type approval) and IEC 61730 (safety qualification) series to represent environmental and operational stress conditions in the field. The National Renewable Energy Laboratory developed the Qual Plus test method [5], which consists of a pair of extended testing sequences, which may be more likely to induce wear-out mechanisms and failures observed in fielded modules. Relative to the IEC 61215 protocol, Qual Plus recommends an increase in the total number of TC from 200 to 500 in one sequence and adds 1000 DML cycles for the UV-TC50-HF10 (UV, thermal cycle, and HF) sequence, among other changes.

Solder bond interconnection damage because of thermal cycling was determined to be the dominant degradation mechanism in PREDICTS2 test modules and fielded modules that were aged in the natural environment for approximately 6 years at the commercial plant in the U.S. Southwest [6]. EL imaging revealed that busbar defects – lower carrier concentration along the length of cell busbars – was the only type of defect with a notable correlation with series resistance (Rs) [6], and the condition was more prevalent in modules with higher TC exposure. Neither IEC 61215 nor Qual Plus capture backsheet failures or inner layer cracks that lead to solder joint corrosion and submodule faults. Independent qualification of components, particularly UV irradiation exposure for backsheet and encapsulant materials, is needed to reveal potential field failures [1].

Based on I–V curves, fielded modules at the commercial PV plant appeared to have both current loss and increased Rs, likely because of a combination of encapsulant browning, busbar defects, and cell cracks. Examples are shown in Figs. 2 and 3. Modules aged indoors had minimal change in short circuit current (I_{sc}) and open circuit voltage (V_{oc}). Furthermore, modules exposed to mechanical loading stress in the lab had more busbar-related losses and a more significant current drop than modules that were not exposed to mechanical loading [7]. This is consistent with higher degradation in fielded modules that were observed to have higher defect counts. A defect pattern along busbar tabbing wires between cells was detected using EL imaging.

The linkage between cracked PV cells and long-term reliability has become an important topic for researchers and industry. Common qualification test sequences performed on new PV modules suggest that cracks have minimal impact on power loss, depending on cell interconnect method [8]. However, results from real-world installations suggest that there is a relationship between the number and type of cell cracks and degradation rate [9]. Evidence also suggests that cracks may have delayed effects, causing negligible changes in performance for several years before annual degradation rates increase sharply and hot spots form [10]. While existing imaging techniques can identify crack type, length, and orientation, little is known about how crack characteristics change with temperature and loading, crack width, the relative movement of fragments within the module laminate, and other fine displacements. While the PREDICTS2 project included counting of cell cracks and other defects, these

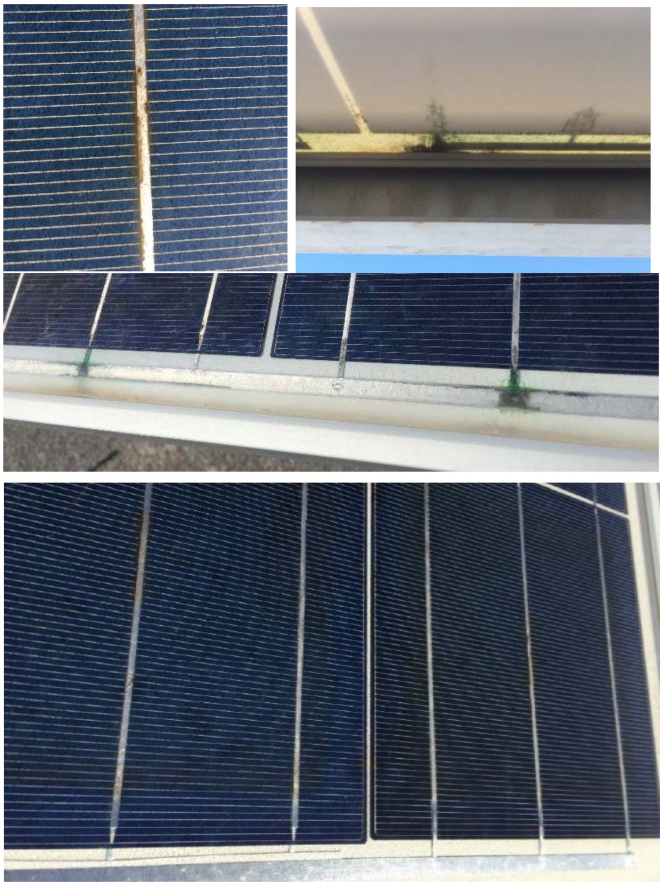

Fig. 2. Examples of busbar and interconnection corrosion and encapsulant browning.

features were not correlated with power loss until now. Improved knowledge of crack impacts is expected to reduce lifetime PV plant performance uncertainty, support development of crack thresholds for PV plants, and inform new module design.

III. Methodology

A. PREDICTS2 Accelerated Testing

Upon arrival at the SSRC, the 36 PREDICTS2 test modules were inventoried, preconditioned outdoors, and characterized using nondestructive evaluation (NDE) techniques – including visual inspection, indoor flash test I–V curve measurements, and EL imaging [1]. Modules were observed to have variations in power rating, backsheet BOM, and encapsulant as well as unique defects and manufacturing signatures. Samples were all 72-cell modules; 34 modules had 290-W_p nameplate rating, and two modules were rated 285 W_p.

Fig. 4 shows the number of modules for each accelerated test sequence, the process flow, NDE events (labeled "I–V Test"), and the on-sun exposure time in the humid subtropical environment after all accelerated tests were complete. Twelve modules followed the standard IEC 61215 test sequences (top two rows), and 24 modules followed the Qual Plus test sequences (bottom two rows). All of the tests begin with outdoor preconditioning of PV modules at the required on-sun exposure equivalent to

Fig. 3. Example EL image of module with multiple cell cracks (red) and busbar defects (blue).

5 kWh/m^2. The HF tests for both test procedures include UV preconditioning of the modules with 15 kWh/m^2 using a combination of UV-A and B irradiance. The modules undergo 50 TC (−40 °C to 85 °C) and 10 HF (−40 °C to 85 °C at 85% humidity) cycles for IEC 61215, whereas the Qual Plus procedure adds 1000 DML (±1000 Pa, 1 to 10 cycles/minute) cycles before the TC50HF10 test. The IEC 61215 procedure includes 200 cycles for the TC test sequence, and the Qual Plus includes 500 cycles. While the wet current leakage test is part of both test procedures, it was not performed in this study. Modules installed on sun were equipped with microinverters and connected to the grid.

The NDE measurements were the basis for determining module performance before and after the accelerated aging process. The module I–V curve measurements after outdoor preconditioning (T0) and after the accelerated aging tests (T1) were taken using an indoor flash tester at the standard test condition (STC) (25 °C module temperature, 1000 W/m^2 irradiance, and AM1.5 spectrum). The flash tester was calibrated by the manufacturer

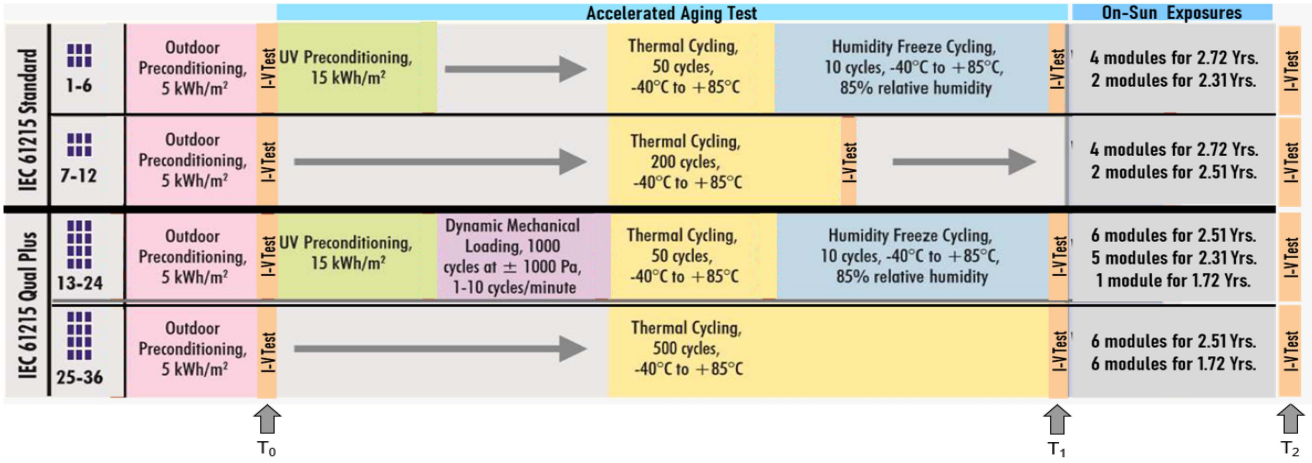

Fig. 4. PREDICTS2 process flow for accelerated aging test sequences and on-sun exposure of the 36 PV test modules.

prior to use in this project. Core Energy Works used an outdoor I–V tester, Solmetric PVA-1500, to take final I–V measurements (T2) in the natural operating condition for on-sun modules. They performed custom calibration and postprocessing of the Solmetric PVA-1500 measurements. Data were translated to STC for analysis. Prior to measurement, each module was cleaned to remove the impact of soiling from the measured values. Uncertainty because of use of different I–V test devices was not considered in the analysis.

Two issues were encountered with the PREDICTS2 performance data. During accelerated aging of the second batch of Qual Plus modules, LabVIEW crashed following an environmental chamber equipment failure, and the modules were not subjected to a forward bias at temperatures above 25 °C, as specified by the test procedure. Instead, modules experienced open-circuit conditions during the entire test period. The second issue occurred when the second batch of Qual Plus modules completed testing. The team determined that there had been a calibration issue with the flash tester, leading to incorrect temperature adjustments to STC. To correct the issue, it was necessary to translate and reanalyze the raw I–V curve data (initial and final measurements) for all 36 modules. The process developed for I–V curve smoothing, translation, and feature extraction was implemented in Python programming language [1].

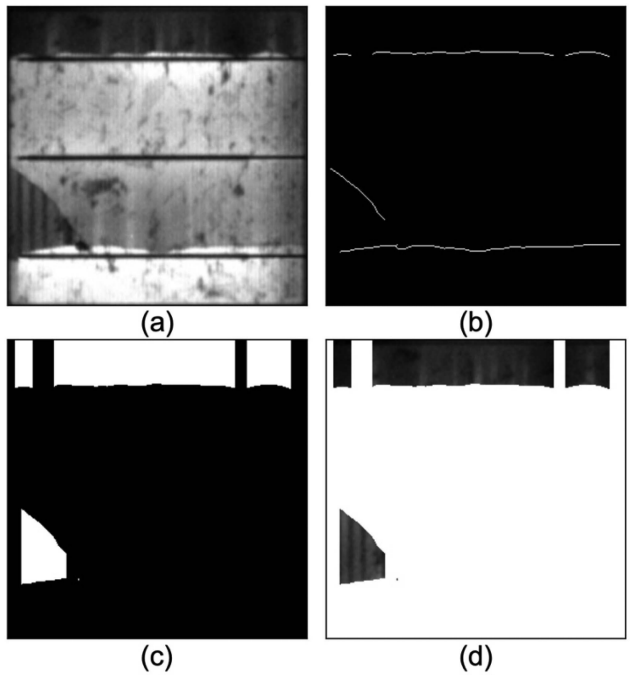

Fig. 5. Example of feature extraction steps to determine worst-case inactive area because of cell cracks. (a) Cell image cropped from module image. (b) Cracks detected by PV-Vision with width of at least one pixel. (c) Isolated area caused by cracks. (d) Isolated area in the original cell image. The mean grayscale value of the original image is considered a descriptor for cracks.

B. Cell Crack Analysis

Cracks shown in EL images taken at times T0, T1, and T2 were quantitatively analyzed with PV-Vision [11], an open-source computer vision tool for EL image analysis developed in the DuraMAT project. However, in-field EL images taken at T2 had higher noise than the dark room EL images obtained at T0 and T1, which negatively affected the performance of PV-Vision. The automated analysis at T2 was determined not to be reliable, and therefore, only T0 and T1 crack data are presented. PV-Vision utilized a trained deep learning model to first segment the cracks from EL images and subsequently calculate various crack features. Algorithms were then used to estimate the maximum inactive area that may occur if cracked portions of cells become isolated. Features of cracks, such as crack length and relative brightness of isolated and nonisolated areas were then correlated with power loss.

Four crack features were explored: cumulative crack length (L), the proportion of area isolated by cracks (PA), brightness (normalized mean grayscale value G) of the whole cell image (G1), and brightness (normalized mean grayscale value G) of isolated areas caused by cracks (G2), as shown in Fig. 5. Fig. 5(a) is an example of a cell image with a spatial resolution of 0.55 mm/pixel. Fig. 5(b) shows the detected cracks with width of

at least one pixel, and Fig. 5(c) shows the worst-case inactive area because of cell cracks, PA, assuming this area becomes totally isolated and charge carriers generated in it cannot flow to the busbars. As not all such areas will be electrically disconnected in practice, Fig. 5(d) is the isolated area in the cell image used to calculate G2. To normalize pixel intensities, we assume that the brightest 1% of the module image will not exhibit severe degradation over time. Therefore, we normalized the cell image by dividing the grayscale value of the cell image by the 99-percentile grayscale value of the module in which the cell resides. We note that these features are designed to look at typical descriptors such as total crack length but also examine other effects. For example, a longer crack may not cause a larger isolated area if the crack exists between two busbars and is parallel to them. Also, a larger isolated area may not cause severe power loss if the severity of that isolation is insignificant (i.e., a low G2). The equations to calculate those features are designed as follows:

$$L\,(\text{mm}) = number\ of\ crack\ pixels * 0.55\ \ (\text{mm}) \tag{1}$$

$$PA = \frac{Area_{isolate}}{Area_{cell}} \tag{2}$$

$$G1 = \frac{\sum_{cell} G/G_{module}^{99\%}}{Area_{cell}} \tag{3}$$

$$G2 = \frac{\sum_{isolate} G/G_{module}^{99\%}}{Area_{isolate}}, 1\ if\ no\ isolation. \tag{4}$$

IV. Results and Discussion

Individual modules are denoted by unique markers and colors, so that the performance of each module can be tracked across T0, T1, and T2. Cumulative changes in electrical parameters are labeled as "Total."

A. IEC 61215 TC200 and Qual Plus TC500 Test Comparison

The Qual Plus TC500 test has the same operating protocols as the IEC TC200, except that it has an extra 300 thermal cycles. Fig. 6 shows a comparison of the IEC TC200 and Qual Plus TC500 tests to illustrate the percent change in maximum power (P_{mp}) of the exposed modules relative to the previously measured condition. T1 I–V curve trace measurements taken after completion of indoor aging tests are relative to I–V measurements after module preconditioning (T0). T2 I–V measurements after outdoor exposure are relative to T1. Total cumulative change is relative to T0. Fig. 7 shows the percent change in three I–V parameters, I_{sc}, V_{oc}, and fill factor (FF), that could have contributed to the degradation of P_{mp}.

The modules in the IEC TC200 aging test showed a slight P_{mp} variation of 0.4% to −0.4% at T1 (Fig. 6), whereas the modules in the Qual Plus TC500 aging test showed a greater variation of−0.6% to −4.0% and a median value of −1.6%. A drop in FF for the Qual Plus TC500 modules appears to be the reason for the P_{mp} degradation.

After on-sun exposure (T2), the median P_{mp} of the IEC TC200 modules degraded about −3.5% relative to T1, whereas the median P_{mp} of the Qual Plus TC500 modules exhibited another

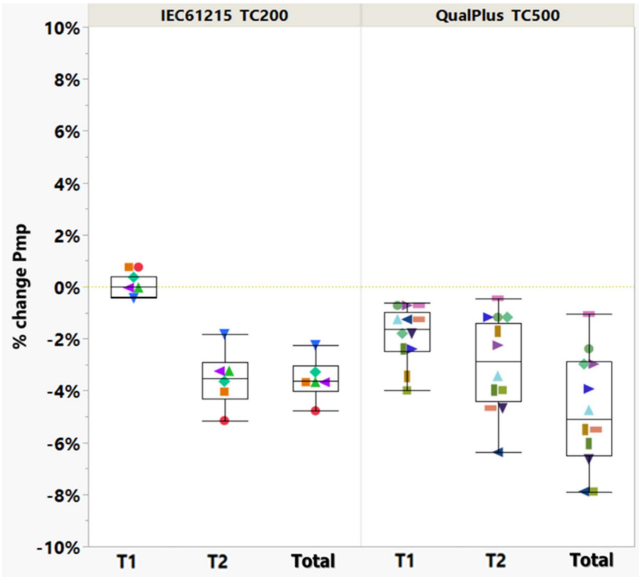

Fig. 6. Percentage change in P_{mp} for IEC 61215 TC200 and Qual Plus TC500 modules after indoor accelerated aging tests (T1), after outdoor exposure (T2), and total cumulative change.

roughly −1.2% absolute drop. This continued degradation during on-sun testing can be attributed to the roughly −4% loss in V_{oc} for both IEC TC200 and Qual Plus TC500 modules. The median Total degradation relative to T0 was −3.6% and −5.1% for the TC200 and TC500 modules, respectively.

B. Comparison of IEC 61215 TC50HF10 and Qual Plus TC50HF10DML1000 Tests

The Qual Plus TC50HF10 test has the same operating protocols as the IEC TC50HF10, except that it adds 1000 DML cycles. Fig. 8 shows a comparison of P_{mp} for IEC TC50HF10 and Qual Plus TC50HF10DML1000 modules after completion of accelerated tests (T1). Fig. 9 shows the percent change in I–V parameters that potentially contributed to the degradation of P_{mp}.

The modules in the IEC TC50HF10 aging test showed a 0.6% to −1.4% P_{mp} variation relative to initial values (Fig. 8) because of −6.3% reductions in FF (Fig. 9). The large variation in FF is compensated for by a 6.8% increase in I_{sc}. Similarly, modules in the Qual Plus TC50HF10DML1000 aging test showed a median decrease in P_{mp} of −1.7% at the end of the indoor accelerated test (T1) (Fig. 8) because of a −4.2% drop in FF, which was partly compensated for by a 3.6% rise in I_{sc}.

During on-sun exposure (T2), the median P_{mp} of the IEC TC50HF10 modules fell −2.2%, while the median P_{mp} of the Qual Plus TC50HF10DML1000 modules rose by about 1% absolute (Fig. 8). While V_{oc} fell during outdoor exposure, FF rose to compensate (Fig. 9).

C. Degradation Because of IEC 61215 and Qual Plus Tests

The PREDICTS2 modules that endured the IEC TC50HF10 accelerated aging tests showed a median −0.2% change in power between T0 and T1, and the modules that endured the IEC TC200

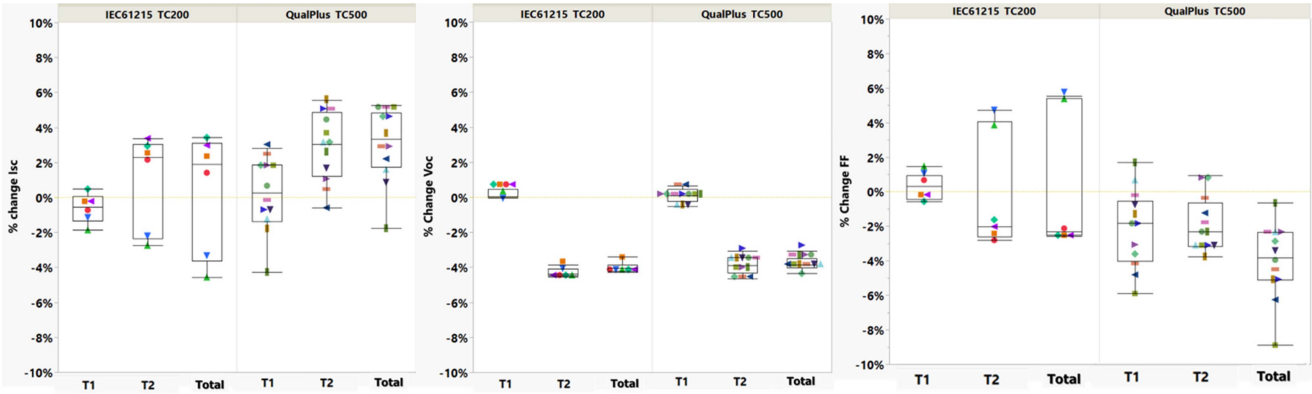

Fig. 7. Percentage change in module electrical parameters (I_{sc}, V_{oc}, and FF) for IEC 61215 TC200 and Qual Plus TC500 modules after indoor accelerated aging tests (T1), after outdoor exposure (T2), and total cumulative change.

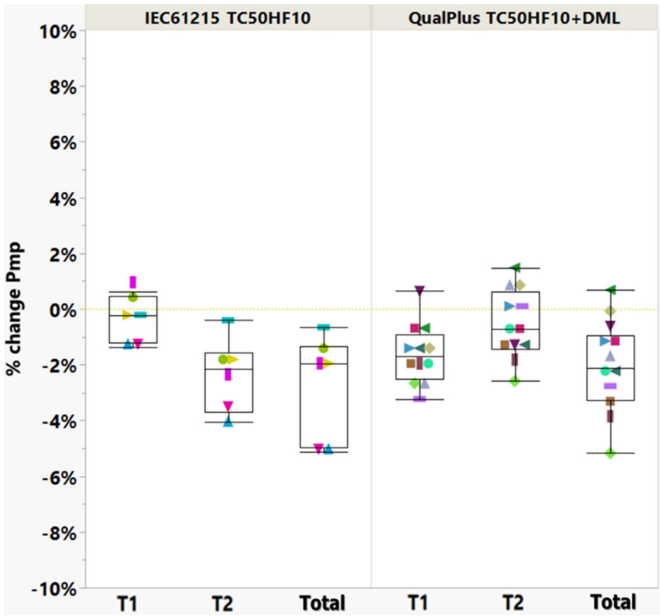

Fig. 8. Percentage change in P_{mp} for both IEC 61215 TC50HF10 and Qual Plus TC50HF10DML1000 test sequences after indoor accelerated aging tests (T1), after outdoor exposure (T2), and total cumulative change.

accelerated aging test showed almost no change in power, as shown in Fig. 10.

The modules in the two legs of the Qual Plus accelerated aging tests also had similar changes in P_{mp} at T1. TC50HF10DML1000 modules showed a median -1.7% drop in P_{mp}, and TC500 modules had a median -1.6% drop. The change in P_{mp} for all test protocols was within the 5% threshold, as shown in Fig. 10.

D. Degradation Because of On-Sun Exposure

After on-sun exposure (T2), IEC TC50HF10 modules exhibited a median change in P_{mp} of -2.2%, whereas IEC TC200 modules exhibited a slightly higher drop of -3.5% (Fig. 11).

The change in the two legs of the Qual Plus tests was more pronounced. TC50HF10DML1000 modules exhibited a median change in P_{mp} of only -0.7%, whereas TC500 modules exhibited a median change of -2.9%.

E. Power Loss in Modules Related to Accelerated Aging Test Correlated to Cell Cracks Obtained From EL Imaging

Crack features for each of the 36 PREDICTS2 modules were calculated based on the mean crack values of the cells. Those module crack values were correlated with the module I–V parameters at T0 and T1 using the Spearman correlation coefficient, as shown in Fig. 12. The x-axis of each plot on the left shows the change in crack features over the time periods, and the y-axis is the change in I–V parameters. All changes are calculated relative to T0. The heatmap on the right side of Fig. 12 shows the correlation coefficient between I–V parameters and crack features. It demonstrates that crack features L, PA, and G2 have a high correlation with P_{mp}. PA shows a relatively lower correlation, possibly because isolated regions with low crack resistance may have negligible power loss.

Fig. 13 shows the change in important crack features (L, PA, and G2) over time in the different aging test sequences. For modules in the IEC test sequences, the changes in the three crack features are negligible at T1. Conversely, modules in the Qual Plus test sequences have more obvious changes in isolated cell area and more severe crack growth. Qual Plus TC500 caused a greater change in G2 but subtle changes in total crack length, L, and worse-case isolated area, PA. These findings denote that thermal cycling influences the disconnection of existing isolated areas (i.e., crack resistance) more than crack growth. Wearing of metal contacts that bridge cracks is a possible mechanism known to occur during thermal cycling. On the other hand, the mechanical loading cycles in Qual Plus TC50HF10DML1000 yielded both more severe cracks by expanding the isolated area through crack growth, as well as worsening the disconnection of isolated areas. This analysis of quantified cell crack features implies that applying higher numbers of thermal cycles may be useful in evaluating module susceptibility to metallization wear, and DML can be utilized to evaluate potential for crack growth.

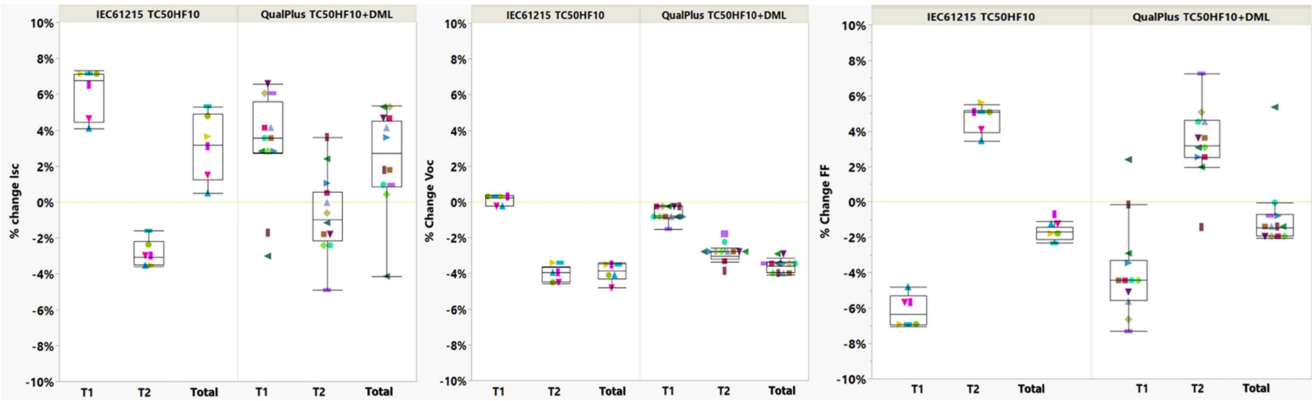

Fig. 9. Percentage change in module electrical parameters for IEC 61215 TC50HF10 and Qual Plus TC50HF10DML1000 modules after indoor accelerated aging tests (T1), after outdoor exposure (T2), and total cumulative change.

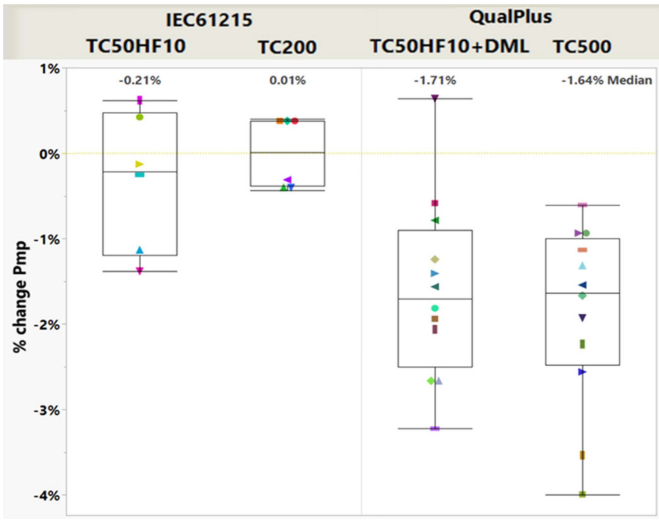

Fig. 10. Percentage change in P_{mp} for all modules after indoor IEC 61215 and Qual Plus accelerated aging tests (T1).

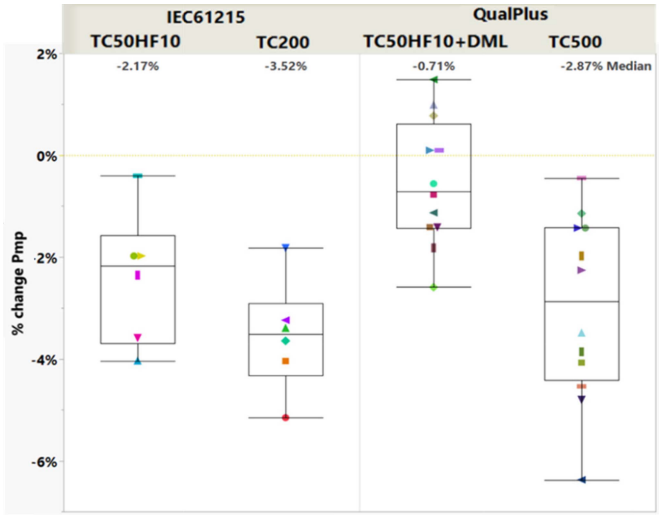

Fig. 11. Percentage change in P_{mp} for all modules after outdoor exposure (T2) relative to condition after completion of IEC 61215 and Qual Plus test sequences (T1).

F. Insights on Accelerated Aging Protocols

Accelerated testing results can be used to inform development of future test protocols. The following insights on protocol strengths and deficiencies were developed based on the broader project results and observations and go beyond the focus of this article:

1) *Thermal cycling.* A linear relationship between thermal cycling and Rs for indoor tests with TC200 and TC500 was extrapolated to accurately predict Rs in fielded modules after about 6 years of exposure [6], [12], [13]. TC200 and TC500 exposures were equivalent to about 2 years and almost 5 years, respectively, in the outdoor environment at the U.S. Southwest plant location. While these results are valid for the specific module type, plant location, and exposure period studied in this project, they suggest that extended thermal cycling durations may provide insights on long-term Rs. The difference in brightness of isolated areas for TC200 and TC500 modules suggests that thermal cycling increases disconnection. Extended thermal cycling tests could provide further insights on degradation in modules containing cell cracks and metallization durability.
2) *Dynamic mechanical loading.* DML stress applied indoors for Qual Plus modules produces more busbar-related defects and more significant drop in current than was observed in IEC 61215 modules that did not receive DML. This finding is consistent with higher observed degradation in fielded modules that also have higher defect counts, but a direct comparison between indoor and outdoor results has not been performed. DML was associated with both increased crack growth and greater disconnection of isolated cell fragments. Effects on cell crack features could be further explored by changing the pressure level and number of cycles.
3) *UV irradiation.* Subsets of fielded modules with 6 years of outdoor exposure were observed to have backsheet cracking (polyamide), inner layer cracking (PET), and submodule faults (PET). Modules in the TCHF legs of the IEC 61215 and Qual Plus test sequences receive

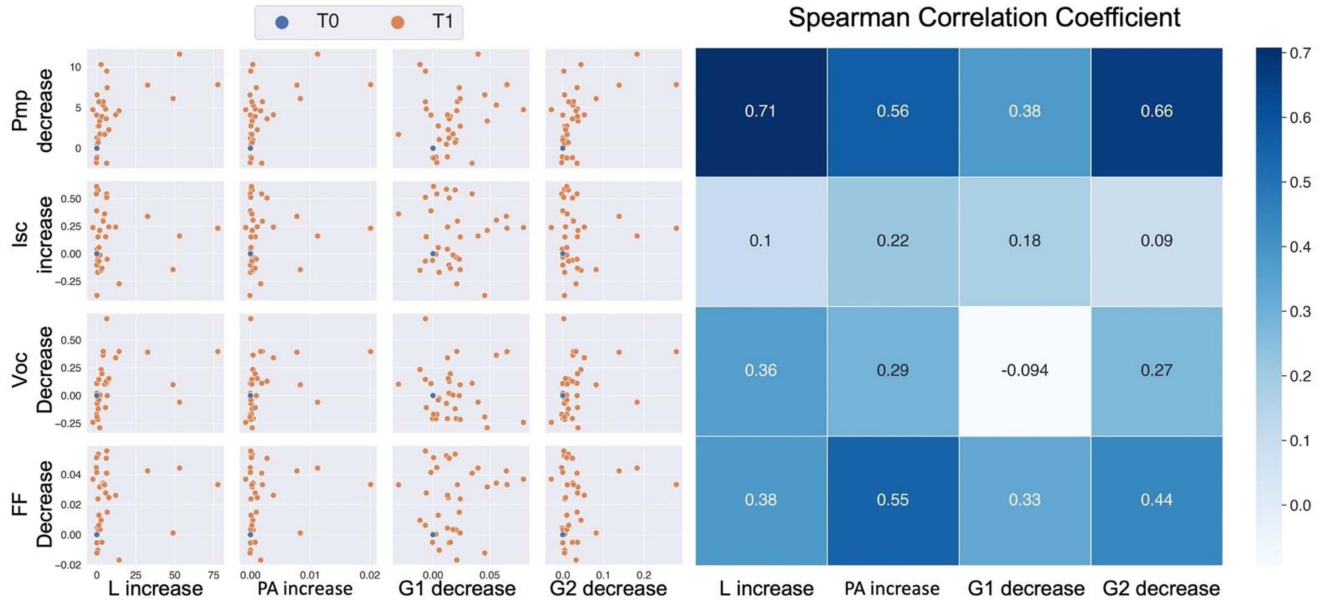

Fig. 12. Correlation between I–V parameters and crack features for all 36 PREDICTS2 modules. The left scatterplot shows the I–V parameters as a function of crack features over time. The right heatmap shows the corresponding Spearman correlation coefficients between the I–V parameters and crack features.

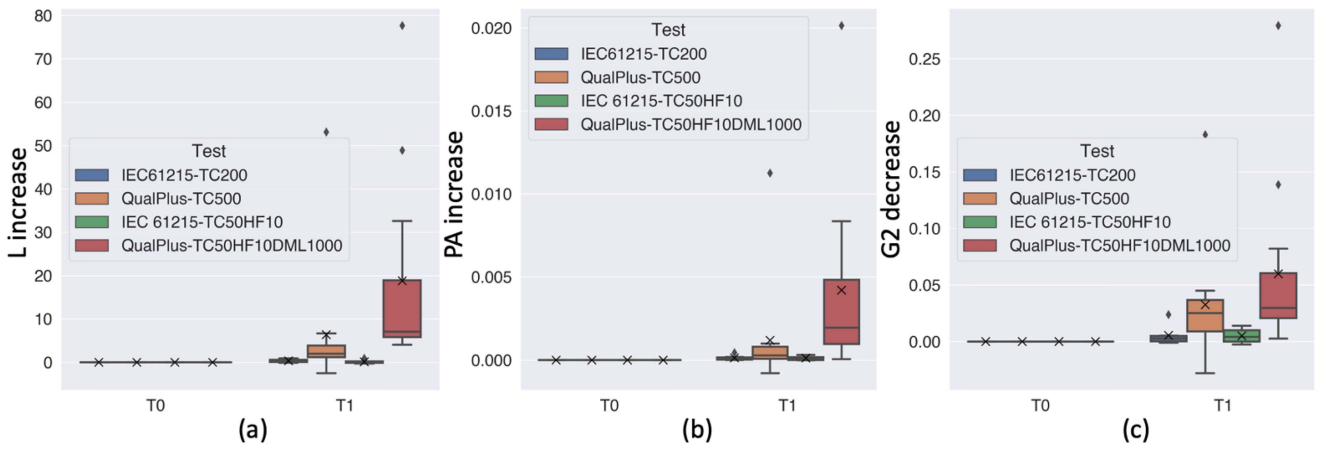

Fig. 13. Change of crack features under IEC and Qual Plus test sequences over time, where "x" in the boxplot denotes the mean value. (a) Crack length. (b) Proportion of isolated area. (c) Mean grayscale value of isolated area.

15-kWh/m^2 UV exposure on the front side of the module, but it is not sufficient to emulate UV exposure to the backsheet. As a result, these degradation/failure modules were not observed in accelerated-aged modules. UV exposure and related testing should be considered for subcomponents of modules, such as backsheets and encapsulants. This should be done in such a way that failures such as polyamide backsheet cracking and PET backsheet inner layer cracking can be predicted. In addition, extended UV exposure on encapsulant coupons or minimodules may allow for predictions of encapsulant transmission losses over time and resulting impacts to I_{sc} and current at maximum power (I_{mp}).

4) *Power loss.* Qualification tests do not induce the level of degradation observed in modules with 6 years of outdoor exposure, and the presence of additional environmental stressors outdoors makes it challenging to use qualification tests to predict power loss. Fielded modules exhibit current loss and increased Rs, likely because of a combination of encapsulant browning, busbar defects, and cell cracks, whereas modules aged indoors have minimal change in I_{sc} and V_{oc}. Maximum power point voltage (V_{mp}) changes in accelerated-aged modules were because of increases in Rs.

V. Conclusion

This article investigated the change in electrical parameters and effects of cell cracks for 36 PV modules split between four different accelerated aging test sequences (two legs of IEC 61215 and two legs of Qual Plus). Module reductions in P_{mp} were all less than the 5% threshold for both the IEC 61215 and Qual Plus test protocols. The TC200 accelerated aging test

resulted in no measurable change in PV module power output, while subsequent on-sun testing resulted in a -3.5% drop in P_{mp} because of a decrease in V_{oc}. TC50HF10 modules had a -1.4% drop in P_{mp} following the accelerated aging tests, and a slight rise during the outdoor exposure period. For the Qual Plus modules, the P_{mp} dropped -1.6% during the accelerated testing because of FF loss and another -1.2% drop outdoors because of V_{oc} loss. The TC50HF10DML1000 modules had a similar median P_{mp} drop of -1.7% during indoor accelerated tests because of FF, followed by a slight rise during outdoor testing.

Different performance degradation trends were identified during accelerated aging tests and on-sun testing. FF loss was the common cause for the observed decrease in power output during the accelerated aging tests, while decreases in both V_{oc} and FF dominated the power loss during on-sun exposure. A substantial tradeoff between I_{sc} and FF indicated nonuniform degradation among module cells in the TCHF test sequences for both the IEC 61215 and Qual Plus protocol modules.

Crack effects were quantified with the computer vision tool PV-Vision. Crack features including crack length (L), isolated areas caused by cracks (PA), and brightness of the isolated areas (G2), present high correlation with P_{mp}. By comparing the change of those crack features between modules in the IEC and Qual Plus tests, we found that modules that endured the Qual Plus tests, and particularly the modules that endured mechanical loading, had the highest growth in cumulative crack length and the greatest increase in disconnection of isolated areas. Thermal cycling also reduces current flow to isolated areas but has an insignificant effect on expanding the isolated area. Longer duration thermal cycling tests and DML at different pressures and number of cycles may be useful in evaluating long-term crack behavior.

A unique aspect of the study was the ability to compare electrical parameter variations in fielded modules with 6 years of exposure with modules that were exposed to different accelerated test sequences. Insights on the IEC 61215 and Qual Plus test protocols and the ability to understand, and potentially predict, degradation mechanisms and power loss can be used to inform development of future test protocols.

ACKNOWLEDGMENT

The authors would like to thank Babak Hamzavy for conducting the accelerated aging and outdoor exposure testing in Birmingham. Birk C. Jones at Sandia National Laboratories was instrumental in developing an algorithm to smooth and translate the I–V curve data used in the analysis. Finally, Mason Reed at Core Energy Works obtained final in-field I–V curve traces and EL images, which enabled time-series analysis of cell crack features and effects on PV module power loss. The views expressed in this article do not necessarily represent the views of the DOE or the U.S. Government. The U.S. Government retains and the publisher, by accepting this article for publication, acknowledges that the U.S. Government retains a nonexclusive, paid-up, irrevocable, worldwide license to publish or reproduce the published form of this work, or allow others to do so, for the U.S. Government purposes.

REFERENCES

[1] Improving Solar PV Degradation Prediction Certainty: PREDICTS2 Final Report. EPRI, Palo Alto, CA, USA, 2019, 3002015507.

[2] International Electrotechnical Commission, Terrestrial photovoltaic (PV) modules - Design qualification and type approval, Geneva, Switzerland, 2016.

[3] C. R. Osterwald and T. J. McMahon, "History of accelerated and qualification testing of terrestrial photovoltaic modules: A literature review," *Prog. PV: Res. Appl.*, vol. 17, no. 1, pp. 11–33, 2009.

[4] D. Jordan, T. Silverman, J. H. Wohlgemuth, S. Kurtz, and K. T. VanSant, "Photovoltaic failure and degradation modes," *Prog. Photovolt.: Res. Appl.*, vol. 25, no. 4, pp. 318–326, 2017.

[5] S. Kurtz et al., "Photovoltaic module Qualification Plus testing," National Renewable Energy Laboratory, Golden, CO, USA, 2013.

[6] C. B. Jones, W. B. Hobbs, C. Libby, T. Gunda, and B. Hamzavy, "Predicting photovoltaic module series resistance based on indoor-aging tests & thermal cycling cumulative exposure estimates," in *Proc. IEEE 46th Photovolt. Specialist Conf.*, 2019, pp. 2554–2560.

[7] W. B. Hobbs, B. Hamzavy, C. B. Jones, C. Libby, and O. Lavrova, "In-field electroluminescence imaging: Methods, comparison with indoor imaging, and observed changes in modules over one year," in *Proc. IEEE 7th World Conf. Photovolt. Energy Convers. (Joint Conf. 45th IEEE PVSC, 28th PVSEC 34th EU PVSEC)*, 2018, pp. 3257–3260.

[8] J. Rand and M. Reed, "Rough handling of silicon modules," in *Proc. NREL PV Rel. Workshop*, 2018, p. 1.

[9] N. Shiradkar, "Key results from all India survey of PV module reliability: 2016," in *Proc. NREL PV Rel. Workshop*, 2018, p. 1.

[10] D. Jordan, T. Silverman, B. Sekulic, and S. Kurtz, "PV degradation curves: Non-linearities and failure modes," *Prog. Photovolt: Res. Appl.*, vol. 25, pp. 583–591, 2017.

[11] X. Chen, github: pv-vision. p. 14. [Online]. Available: https://github.com/hackingmaterials/pv-vision

[12] C. B. Jones, B. Hamzavy, W. B. Hobbs, C. Libby, and O. Lavrova, "IEC 61215 qualification tests vs outdoor performance using module level in situ I–V curve tracing devices," in *Proc. IEEE 7th World Conf. Photovolt. Energy Convers. (Joint Conf. 45th IEEE PVSC, 28th PVSEC 34th EU PVSEC)*, 2018, pp. 1286–1291, doi: 10.1109/PVSC.2018.8548222.

[13] C. B. Jones, T. Karin, A. Jain, W. B. Hobbs, and C. Libby, "Geographic assessment of photovoltaic module environmental degradation stressors," in *Proc. IEEE 46th Photovoltaic Specialist Conf.*, 2019, pp. 1346–1351, doi: 10.1109/PVSC40753.2019.8980741.